Ocean Sci. Discuss., 7, 445–475, 2010
www.ocean-sci-discuss.net/7/445/2010/

Ocean Science Discussions

This discussion paper is/has been under review for the journal Ocean Science (OS).
Please refer to the corresponding final paper in OS if available.

Upper layer current variability in the Central Ligurian Sea

P. Picco[1], A. Cappelletti[2], S. Sparnocchia[3], M. E. Schiano[4], S. Pensieri[5], and R. Bozzano[5]

[1]ENEA CRAM, Forte S. Teresa, 19036 Pozzuolo di Lerici (SP), Italy
[2]ENEA, Via V. Viviani 23, 56124 Pisa, Italy
[3]CNR-ISMAR-TS, Viale R. Gessi 2, 34123 Trieste, Italy
[4]CNR ISMAR-GE, Via dei Marini 6, 16149 Genova, Italy
[5]CNR ISSIA-GE, Via dei Marini 6, 16149 Genova, Italy

Received: 20 January 2010 – Accepted: 22 February 2010 – Published: 9 March 2010

Correspondence to: P. Picco (paola.picco@enea.it)

Published by Copernicus Publications on behalf of the European Geosciences Union.

Abstract

Long-time series of surface currents and meteorological parameters were analysed to estimate the variability of the upper layer circulation as a preliminary study of the Ligurian Air-Sea Interaction Experiment (LASIE07). Current meter data were collected by an upward-looking RDI Sentinel 300 kHz ADCP deployed in the Central Ligurian Sea (43°47.77′ N; 9°02.85′ E) near the meteo-oceanographic buoy ODAS ITALIA1 for over eight months. The ADCP sampled the upper 50 m of water column at 8 m vertical resolution and 1 h time interval; surface marine and atmospheric hourly data were provided by the buoy. Currents were mainly barotropic and directed NW, according to the general circulation of the area, had a mean velocity of about 18 cm s^{-1} and hourly mean peaks up to 80 m s^{-1}. Most of the observed variability in the upper thermocline was determined by inertial currents and mesoscale activity due to the presence of the Ligurian Front. Local wind had a minor role in the near-surface circulation but induced internal waves propagating downward in the water column.

1 Introduction

The main scientific goal of the Ligurian Air-Sea Interaction Experiment (LASIE), carried out in the Central and Eastern Ligurian Sea during the summer 2007 (Teixeira, 2007), was the improvement of high-resolution oceanic prediction systems, from the setting up of appropriate monitoring networks to the development of forecasting models. The experiment focused on the oceanic and atmospheric boundary layers, their interactions and variability. The selected experimental area is very suitable for this type of investigation since both atmospheric and marine circulation is greatly influenced by strong air-sea interaction processes occurring over this basin.

The circulation in the Ligurian Sea is characterized by a cyclonic gyre involving both the surface Modified Atlantic Water (MAW) and the lower Levantine Intermediate Water (LIW) (Millot, 1987). The cyclonic circulation affects the hydrological structure of the

OSD

7, 445–475, 2010

basin, giving rise to three distinct zones: the coastal peripheral, the frontal and the central ones. The frontal zone divides the warmer and lighter coastal waters from the colder and denser waters of the central zone (Sournia et al., 1990). Although this structure is almost permanent, it shows an important seasonal and inter-annual variability and intense mesoscale activity related to the strong frontal system (Astraldi and Gasparini, 1992; Vignudelli et al., 2000). The two main current systems entering the Ligurian Sea -the Western Corsica Current (WCC) and the Eastern Corsica Current (ECC) – join north of Cape Corse, giving origin to the so-called Northern Current (NC) which flows along the Ligurian and French coasts.

Despite of the existence of long-term current measurements in the coastal Ligurian Sea (e.g. Astraldi and Manzella, 1983), there is a lack of background knowledge on the high frequency current variability in the open sea. In order to investigate the surface current variability and its response to the local atmospheric forcing, a mooring equipped with an upward-looking ADCP (Acoustic Doppler Current Profiler) and CTD sensors was deployed on September 2003, offshore, near the meteo-oceanographic buoy ODAS ITALIA1 (Picco et al., 2007). The results of the analysis of the long-time series of data collected from this mooring and from the buoy are given in this paper. Although the period of observation does not overlap with that of the LASIE, a preliminary assessment of the variability in the area of the experiment can be of advantage for a more comprehensive interpretation of the obtained results.

The paper is organised as follow: Sect. 2 presents the experimental set-up and the available data. A brief description of the meteorological and hydrological conditions occurring during the examined period is reported in Sect. 3. In Sect. 4 the surface currents are investigated by using both EOF and time-frequency analysis, while Sect. 5 focuses on the effects of local wind. The main findings are summarized in Sect. 6.

OSD
7, 445–475, 2010

2 Data

ADCP current data were collected by an oceanographic mooring deployed in the Central Ligurian Sea (43°47.77′ N; 9°02.85 E) at 1040 m depth from 13 September 2003 to 25 May 2004. It was composed by an upward-looking broadband RDI 300 kHz ADCP located at 58 m depth and by two SBE-SeaCat 37 temperature and conductivity probes installed at 68 m and 250 m depth. The probe at 68 m was also equipped with a pressure sensor to monitor the instrument depth, but it stopped working on 11 April 2004.

The ADCP was set-up at 8-m vertical resolution; the mid-depth of the first bin cell was at 48 m and the last (bin 6) at 8 m, close to the sea-surface. The sampling time interval was 1 h and each data ensemble was the average of 55 pings; the estimated nominal error on the horizontal currents was 0.23 cm s^{-1}. The vertical displacement of the mooring was checked using both the pressure measurements from the SBE and the distance of the ADCP from the water surface computed according to Visbeck and Fischer (1995). The two estimations were in good agreement and indicated that the mooring was generally stable: vertical displacements higher than 4 m only occurred during a few short events. Pitch and roll data never exceeded 2.5°, below the 9° indicated by the manufacturer (Gordon, 1996) as the limit for tilt compensation. Echo amplitude, which describes the relative strength of the backscattered signal, was strong enough to maintain the signal/noise ratio above 10 during almost all the period of measurements (Schott and Leaman, 1991). The mean profile had a maximum for bin 6, and some attenuation with the distance from the instrument. Percent of good data was always near 100%, so there was no need to remove any data.

Meteorological data were provided by the open sea laboratory ODAS ITALIA 1. It is a spar meteo-oceanographic buoy specifically developed for air-sea interaction studies and equipped to collect meteorological and marine data. In the period referred to, it was moored about 40 nautical miles offshore, in the Central Ligurian Sea (43°47.28′ N; 9°09.78′ E) at 1440 m depth (Fig. 1). Two complete sets of meteorological sensors were installed on the top of the buoy at a height of 13.5 m; marine sensors were mounted

OSD
7, 445–475, 2010

along the buoy's body at various depths (0.5, 12, 20, 28, 36 m) to collect sea temperatures and salinity data (see Table 1 for instrumental details). Every 5 s the on board system acquired the meteorological parameters, while marine data were sampled each 30 min. All the collected data were stored on board and transmitted each hour to the receiving station ashore. The buoy operated regularly from 13 September 2003 to 8 March 2004. Only two interruptions, lasting a couple of hours and due to maintenance activities on the buoy, occurred during the experiment. The resulting short gaps were filled with interpolated data.

SBE probes were calibrated at NATO Undersea Research Centre (NURC) in La Spezia before their use and, apart from the above mentioned failure of the pressure sensor, they correctly worked during the entire experiment.

Additional CTD profiles were performed during the mooring deployment and recovery operations on September 2003 and May 2004.

3 Meteorological and hydrological conditions

Hydrological conditions were inferred from the measurements of conductivity and temperature sensors located on the buoy and on the mooring and from the CTD profiles performed during the oceanographic campaigns.

The seasonal evolution of the upper layer during the period of measurements included the late summer stratification, the thermocline erosion, the winter mixing and the formation of weak early spring stratification. The vertical structure, as deduced from CTD profiles taken during the mid September cruise, could be described as a two layer system with the sharp thermocline located around 35–40 m, at the same depth of the subsurface summer minimum salinity (37.85 psu). The upper 25–30 m layer was quite well mixed having 22.5 °C temperature and 38.3 psu salinity. Summer 2003 was one of the hottest in recent years (e.g. Sparnocchia et al., 2006) and in September the sea surface temperature was still very high. Below the thermocline the temperature was near 13.5 °C. Until late autumn, temperature and salinity time series at 35 m depth

(Fig. 2) showed variations up to 4 °C and 3 psu respectively, indicating the alternative presence of the colder and fresher WCC and the warmer and saltier ECC. These episodes, due to the mesoscale dynamics of the front, lasted up to several days. In winter the displacement of the Ligurian Front was detectable only in the deeper layers.

Mixed layer reached the depth of 35 m at the end of October, as a result of the mixing due to the intense (>18 m s^{-1}) westerly wind event. Winter homogeneity was completely developed from mid February when temperature was below 14 °C, salinity was quite uniform around 38.2 in the upper 70 m and density had the minimum vertical gradient. This situation was still persisting at the beginning of March, when the CT probes installed on the buoy stopped working. CTD profiles taken at the end of April 2004 – just before mooring recovery – indicated an early thermocline formation due to surface warming: the upper 10 m had a temperature of 16 °C and a weak thermal gradient had started to develop. Salinity still had the minimum at the surface (37.88 psu) and it increased with depth, reaching 38.37 psu at 250 m. A relative maximum of temperature and salinity in the layer between 100 and 150 m revealed the signature of the warmer and saltier waters (13.5 °C and 38.26 psu) coming from the Tyrrhenian Sea.

Wind was generally low; wind strength values less than 5 m s^{-1} (force 3) occurred in the 50% of the cases. Both wind speeds and directions showed high variability (Fig. 3): mean speed on the whole period of observation was 6.2 m s^{-1} and the standard deviation was 4.1 m s^{-1}. Wind strength greater than 13 m s^{-1} (force 7) occurred only for 5% of the time and, generally, during the passage of significant low systems (pressure minimum below 1000 hPa) with westerly wind. The maximum hourly mean value (23.3 m s^{-1}) was recorded on 5 October during the passage of a low (minimum of 995 hPa). Only in a few cases the high wind persisted longer than 48 h, in particular during 22–24 January when the wind was blowing from NE at a speed higher than 10 m s^{-1}.

OSD
7, 445–475, 2010

4 Currents analysis

4.1 General description

During the period of observation, the currents were almost vertically homogeneous and mainly directed northwest, following the general cyclonic circulation of the Ligurian Sea. The mean speed decreased with depth from 20.8 cm s^{-1} in the surface layer to 13.9 cm s^{-1} at 48 m (Table 2). The flow was shifted northeastern by meanderings associated to the mesoscale activity with a periodicity of about ten days (Figs. 4–5). Currents directed to the South were observed only during a few short episodes; they had a lower intensity and were mainly confined to the near-surface layer, where meandering and rotations were more developed (Fig. 6). This difference in the pattern was consistent with the results of the complex correlation analysis (Table 3) which reports lower value coefficients in the first column.

4.2 EOF analysis

Complex Empirical Orthogonal Function (EOF) analysis was performed on the hourly time series (Emery and Thomson, 2001). EOF decomposition is often used to analyse geophysical data characterized by a spatial pattern – in this case the ADCP current profile-evolving with time. The profile at each temporal step is represented as a linear combination of a limited number of profiles (modes) which can be associated to a different dynamical mechanism, while the temporal series of the coefficients indicates the relative importance of each mode.

The first mode profile (Fig. 7) describes the mean northwestern flow and has a mean intensity decreasing from 19.2 cm s^{-1} at the second level up to 12.4 cm s^{-1} at 48 m depth. Near surface current intensity is slightly lower (18 cm s^{-1}) than in the layers below, but it is compensated by the second mode, which reaches the maximum (10 cm s^{-1}) at surface. The second mode describes the surface variability having the highest velocities in the upper layer but negligible values in the other layers. On the

OSD
7, 445–475, 2010

average, the first mode accounts for 0.67 of the total signal, the second for 0.2 and the third only for 0.08, so that three modes are able to reconstruct 95% of the entire signal.

The temporal evolution of each mode current was reconstructed by using the modes profile and the coefficients time series. The progressive vector of each mode in the surface layer are reported in Fig. 8.

Second mode surface currents displayed an irregular pattern with sudden inversions and complete rotations; they were mainly directed southwest until mid January, after then they shifted toward southeast. In a few cases second mode currents were higher than the first mode, in particular during the periods 8–13 November and 23–25 February, in the presence of a southern current.

Third mode currents were smaller than the others, having a mean intensity below 3 cm s^{-1}, further decreasing from the end of December. Only on 30 September and on 13–14 October intensity reached 5 cm s^{-1}.

4.3 Time-frequency analysis

Rotary spectral analysis was performed on current time series at each level, according to Gonella (1972). To investigate the sub-diurnal band, complex FFT analysis was performed on 23 samples 256-h long which were then averaged. Before the analysis, each sample was smoothed in order to limit the effect of the finite-length of the time series, which concentrates energy at the lowest frequency components; then it was detrended to reduce the high-frequency noise. All the six spectra were by far dominated by the inertial frequency, which, at this latitude, is 0.0578 cph (the correspondent period is 17.3 h). The inertial peak had the maximum amplitude (10.8 cm s^{-1}) at the second level and decreased to 6.7 cm s^{-1} at the lowest depth; standard deviation spanned from 8.3 to 4.2 cm s^{-1}. The analysis did not evidence the presence of tidal components, not even in the anticlockwise part, which was not masked by the inertial signal. Only a small relative maximum in the semidiurnal band appeared in the first layer spectrum. The depth-averaged spectrum is shown in Fig. 9. Similar results were obtained by separately analyzing the first two modes. In both cases energy was concentrated in

OSD
7, 445–475, 2010

the inertial band, the second-mode positive spectrum evidenced a small peak on the semidiurnal band, which was absent in the first-mode spectrum.

In order to detect the occurrence of inertial motions and to analyse their temporal evolution, time-dependent complex frequency analysis was performed on the time series. The spectrogram was obtained using a 256 h sliding window with 255 h overlap between each sample; a 256 h window Hanning filter was applied to the resulting time series. The time evolution of the energy in the inertial band (5.6413–6.0319×10^{-2} cph) was then extracted (Fig. 10). Inertial oscillations were observed during the whole period of measurements. They occurred in burst lasting up to several days and were better developed in autumn: the more persistent and energetic were observed from 20 November to 6 December. The mean amplitude of inertial currents was about 10 cm s^{-1}, comparable with that of the mean flow. During autumn energy was higher at the lower levels and it was consistent with the mixed-layer formation; during the rest of the period it was maximum at surface and attenuated with depth.

To investigate lower frequencies, spectral analysis was also performed on longer samples (512 and 1024 days) but, due to the limited length of the time series, the confidence level increased. Red-spectrum was a dominant feature; the energy was more concentrated in the clockwise component of the spectrum and in the low-frequency components. In addition to the dominant inertial peak, the analysis indicated some energy also on 80 h and 95 h in the positive side of the spectrum.

4.4 Vertical velocities

Vertical velocities structure was characterized by intermittent burst of oscillations reaching the amplitude of few centimeters per second (up to 10 cm s^{-1} in the upper layer). These episodes generally lasted about 2–4 days and interested the entire sampled water column, but the amplitude attenuated with increasing depth. As well as the horizontal currents, also the vertical components were highly correlated: correlation coefficient spanned from 0.56 to 0.97.

OSD
7, 445–475, 2010

The power spectrum was white with well defined peaks on the diurnal and sub-diurnal bands. The diurnal frequency (0.0147 cpd), which is mainly determined by the daily migration of scattering organisms, dominated, while very few energy was found on the inertial frequency. As suggested by some authors (van Aken et al., 2007) this cannot be surprising since this motion is predominantly horizontal. Other peaks related to internal waves – in particular on 8 and 6 h – were detected, but the short duration of these events and their frequency variability did not allow for a good spectral resolution.

To better investigate the time-spectral characteristics of the observed oscillations, the methodology proposed by Jacobs et al. (2001) resulted appropriate for this purpose. The data contained in a 4-days moving window were fit by least square method with a function consisting in a linear trend and a cosine and sine wave. A relatively fine frequency discretization (df=0.025 cpd) was used to span the band from 2 to 6 cpd; the temporal resolution was determined using a 3-day overlapping windows. The resulting spectrogram (Fig. 11) confirmed the episodic nature of the observed oscillations whose energy was spread over the whole frequency range with a weak concentration on 2.8 cpd and 5.5 cpd waves, roughly corresponding to a period of 9.6 and 4.3 h. This suggested the presence of downward propagating internal waves in response to surface forcing.

5 Local wind and currents

The availability of surface meteorological observation from the ODAS buoy allowed to investigate the role of local forcing on the surface circulation. Currents in the near surface layer have shown in several cases a different pattern from the layers below, which were strongly barotropic. Simple considerations indicate the wind as the main responsible factor for such a variability (Wang and Huang, 2004). Since the second EOF mode described the near-surface variability, the relation between local wind and surface currents was investigated by using the second mode time series. Complex correlation coefficient between wind and second mode current daily mean data was 0.64 and 13° the angle.

To estimate the effects of the wind on the surface circulation, numerical tests were performed with a simple numerical model, integrating the Ekman equations reported below.

$$f u = A_V \frac{\partial^2 v}{\partial z^2} \qquad -f v = A_V \frac{\partial^2 u}{\partial z^2}$$

$$u(0) = \frac{\tau_x}{f A_V}$$

$$u(H) = u(H - \Delta z)$$

$$v(0) = \frac{\tau_y}{f A_V} \qquad v(H) = v(H - \Delta z)$$

$$\text{Stability} = A_v \frac{\Delta t}{\Delta z^2} < 0.5 \qquad \text{Ek\_Depth} = \sqrt{\frac{2A_V}{f}}$$

Vertical resolution (Δz) was 8 m – the same of the ADCP – while the water column depth (H) was 100 m. To ensure the numerical stability the time step was 180 s. Free-slip conditions were imposed at the bottom, to simulate an infinite depth. The turbulence diffusion coefficient (A_v) was chosen constant 0.01 $m^2 s^{-1}$. Under these conditions resulting Ekman depth is 14 m. Wind stress (τ) was computed according to Fairall et al. (1996) by using the data available from the buoy. The minimum wind stress able to induce a mean current of the order of few centimeters per second in an 8 m-thick layer is 0.04 Pa, which is obtained from a wind intensity of about 5 $m s^{-1}$. A constant wind stress of 0.088 Pa – the observed mean wind stress over the whole period of measurements – was firstly considered for the test. Resulting mean current intensity was about 10 $cm s^{-1}$, comparable to the velocity of the second mode. Higher wind stress values were considered, excluding the maximum observed (0.52 Pa) because it lasted for a too short period to significantly affect the circulation. The value 0.35 Pa, obtained

from a wind intensity of nearly 14 m s^{-1}, was chosen as a more realistic case for the area. Such a wind stress causes a drift current of about 25 cm s^{-1} in the upper layer.

Wind rotary spectrum was computed on 256-h long samples, which were then averaged. Energy was higher in the positive part of the spectra, but it was generally noisy and peaks were not well resolved, so it did not clearly reveal the presence of any significant periodicity. Only some energy on the semidiurnal band, ascribed to the breeze regime, was detected, while the inertial frequency, which dominates in the marine currents, never appeared. In order to investigate a lower frequency part of the signal, the analysis was performed on 1024-h long samples. Peaks centered respectively on 52 h and 95 h were evidenced in the positive part of the wind spectrum; in the negative most of the energy was found in the 100–140 h large band. A 4-day periodicity was then common to both wind and second mode currents. Due to the quite different spectral characteristics of the two signals, cross spectrum analysis did not provide additional information.

These results indicate a minor role of the wind-driven currents with respect to the general barotropic circulation, but can explain part of the variability observed in the near-surface currents.

6 Discussion

Surface current observations from an upward looking ADCP moored in the Central Ligurian Sea and meteo-marine parameters from a fixed offshore buoy were used to investigate the dynamics of the upper layer and its variability in response to the local atmospheric forcing.

The vertical structure of the currents in the upper thermocline could be described as a barotropic layer moving Northwest at a mean speed of 17.5 cm s^{-1}. Main differences in the pattern, in particular the occurrence of southward currents, were confined to the near-surface layer. The observed northeast meandering can be explained as pulses of the mean flow, as suggested by Sammari et al. (1995) analysing the Northern Current.

Time-frequency analysis revealed that the main variability was determined by the inertial currents. They had a magnitude comparable with the mean velocity and were detected at all depths, in both the first and second mode signals. They occurred intermittently during the whole period of measurements (September 2003–May 2004) and each time they lasted several days. The more energetic ones were found during autumn, when the thermocline was still well developed, while during winter their amplitude was reduced. Inertial oscillations are very common in the ocean. They can be locally generated at the surface by changes in wind stress or by the rapid transit of a low and can persist for several days. These oscillations propagate energy far from the area of generation as well as downward in the water column, generating higher-frequency internal waves through non linear interactions (D'Asaro, 1985; Petrenko, 2003; Pluedelmann and Farrar, 2006). For their contribution to the mixing, they are of particular importance in regions such as the Ligurian Sea, since they compensate the lack of the tidal mixing. The analysed time series did not reveal any clear relationship between the onset of inertial currents and local atmospheric forcing variation, except for the strong wind episode occurred on 6 October. In particular, no evident response to high wind stress variations could be observed during winter months. The existence of mixed layer inertial currents unrelated to wind forcing was reported by different authors. Van Haren and Millot (2003) found similar results in the Ligurian Sea and gave evidence to the important role of the thermal stratification of waters in the vertical propagation.

While a poor direct relationship was found between local wind and inertial current onset, it was evidenced a nearly one-to-one correspondence between the wind stress relative maximum and the occurrence of vertical oscillations, identified by a maximum of daily standard deviation (Fig. 12). Their amplitude did not seem relate to the intensity of wind stress nor to the vertical stratification, as their vertical structure was independent on the season. A more comprehensive analysis on their origin and contribution to the vertical mixing would require longer time series.

The six-level vertical resolution of the ADCP measurements allowed the use of EOF for the decomposition of current profiles. Although the physical interpretation of the

OSD
7, 445–475, 2010

modes is not always clear (Borzelli and Ligi, 1999), in this case this method has proved to be an efficient tool to separate different characteristics of the circulation. The first mode was used to investigate the dominant large-scale circulation. The second mode evidenced the variability confined to the near-surface layer and was considered appropriate to study the effects of the local wind stress.

Wind-driven currents had a minor contribution to the surface circulation of the area, nevertheless, in a few cases, were comparable to the mean geostrophic component. The computed Ekman currents were consistent with the second mode current speed and had a higher correlation with the wind. Such results are encouraging if we consider the relatively low vertical resolution of the ADCP measurements with respect to the computed Ekman depth and the intensity of the wind forcing in the area.

The vertical thermal structure in the upper thermocline displayed a high variability related to the presence of the Ligurian front, the occurrence of internal waves and the wind mixing. Such variability can be taken into consideration when approaching air-sea interaction studies in this area.

Acknowledgements. The content of this paper is based on the presentation at the Conference "Rapid Environmental Assessment (REA)" held in Lerici on 25–27 September 2007.

We are grateful to Mireno Borghini, CNR ISMAR La Spezia, which was responsible for the oceanographic measurements. Thanks are due to the captain and the crew of N/O URANIA for the support during at sea operations.

References

Astraldi, M. and Manzella, G. M. R.: Some observations on current measurements on the Eastern Ligurian Shelf, Mediterranean Sea, Cont. Shelf Res., 2, 183–193, 1983.

Astraldi, M. and Gasparini, G. P.: The seasonal characteristics of the circulation in the North Mediterranean basin and their relationship with the atmospheric-climatic conditions, J. Geophys. Res., 97(C6), 9531–9540, 1992.

Borzelli, G. and Ligi, R.: Empirical Orthogonal Function Analysis of SST Image Series: a Physical Interpretation, J. Atmos. Ocean. Technol., 16, 682–781, 1999.

D'Asaro, E.: The Energy Flux from the Wind to Near-Inertial Motions in the Surface Mixed Layer, J. Phys. Oceanogr., 15, 1043–1059, 1985.
Emery, W. J. and Thomson, R. E.: Data Analysis Methods in Physical Oceanography, Elsevier Science B.V., 638 pp., 2001.
Fairall, C. W., Bradley, E. F., Rogers, D. P., Edson, J. B., and Young, G. S.: Bulk parameterization of air-sea fluxes for Tropical Ocean-Global Atmosphere Coupled-Ocean Atmosphere Response Experiment, J. Geophys. Res., 101(C2), 3747–3764, 1996.
Jacobs, G. A., Book, J. W., Perkins, H. T., and Teague, W. J.: Inertial oscillations in the Korea Strait, J. Geophys. Res., 106(C11), 26943–26957, 2001.
Gonella, J.: A rotary-component method for analyzing meteorological and oceanographic vector time series, Deep-Sea Res., 19, 833–846, 1972.
Gordon, R. L.: Acoustic Doppler Current Profilers, Principles of Operation, A Practical Primer, RDI, San Diego, 1996.
Millot, C.: Circulation in the Western Mediterranean Sea, Oceanol. Acta, 10, 143–274, 1987.
Petrenko, A.: Variability of circulation features in the Gulf of Lion NW Mediterranean Sea, Importance of inertial currents, Oceanol. Acta, 2, 323–338, 2003.
Plueddemann, A. J. and Farrar, J. T.: Observations and models of the energy flux from the wind to mixed-layer inertial currents, Deep-Sea Res. II, 53, 5–30, 2006.
Picco, P., Bozzano, R., Schiano, M. E., Bordone, A., Borghini, M., Di Nallo, G., Schirone, A., and Sparnocchia, S.: Marine Observing Systems from fixed platforms in the Ligurian Sea, B. Geofis. Teor. Appl., 48, 227–240, 2007.
Sammari, C., Millot, C., and Prieur, L.: Aspects of the seasonal and mesoscale variabilities of the Northern Current in the western Mediterranean Sea inferred from the POLIG-2 and PROS-6 experiments, Deep-Sea Res., I, 42, 893–917, 1995.
Schott, F. and Leaman, K. D.: Observation with Moored Acoustic Current Profilers in the Convection Regime in the Golfe du Lion, J. Phys. Oceanogr., 21, 558–574, 1991.
Sournia, A., Brylinski, J. M., Dallot, S., Le Corre, P., Leveau, M., Prieur, L., and Froget, C.: Fronts hydrologiques au large des cotes francaises : Les sites-ateliers du programme Frontal, Oceanol. Acta, 13(4), 413–438, 1990.
Sparnocchia, S., Schiano, M. E., Picco, P., Bozzano, R., and Cappelletti, A.: The anomalous warming of summer 2003 in the surface layer of the Central Ligurian Sea (Western Mediterranean), Ann. Geophys., 24, 443–452, 2006, http://www.ann-geophys.net/24/443/2006/.

OSD
7, 445–475, 2010

Teixeira, J.: Ligurian Air-Sea Interaction Experiment (LASIE) trial plan, NATO Undersea Research Centre, La Spezia, Italy, 30 pp, http://geos2.nurc.nato.int/lasie07, 2007.
Van Aken, H. M., Van Haren, H., and Maas, L. M. R.: The high-resolution vertical structure of internal tides and near-inertial waves measured with an ADCP over the continental slope in the Bay of Biscay, Deep-Sea Res. I, 54, 533–556, 2007.
Van Haren, H. and Millot, C.: Seasonality of internal gravity waves kinetic energy spectra in the Ligurian Basin, Oceanol. Acta, 26, 635–644, 2003.
Vignudelli, S., Cipollini, P., Astraldi, M., Gasparini, G. P., and Manzella, G.: Integrated use of altimeter and in situ data for understanding the water exchanges between the Tyrrhenian and Ligurian Seas, J. Geophys. Res., 105(C8), 19649–19663, 2000.
Visbeck, M. and Fischer, J.: Sea surface conditions remotely sensed by upward-looking ADCPs, J. Atmosph. Ocean Technol., 12, 141–149, 1995.
Wang, W. and Huang, R. X.: Wind Energy input to the Ekman Layer, J. Phys. Oceanogr., 34, 1267–1275, 2004.

Table 1. Details of available data and instruments used.

Parameter	Platform	Instrument	Height/depth	From/to
Wind speed	buoy	Friedrichs 4020	13.5 m	13 Sep 2003/8 Mar 2004
Wind direction	buoy	Friedrichs 4121	13.5 m	13 Sep 2003/8 Mar 2004
Atm. pressure	buoy	Friedrichs 5006	12.5 m	13 Sep 2003/8 Mar 2004
Sea temperature and conductivity	buoy	SBE SeaCat 37 SBE 39	−0.5, −5, −12, −20, −28, −36 m	13 Sep 2003/8 Mar 2004
Sea temperature and conductivity	mooring	SBE SeaCat 37	−68–250 m	13 Sep 2003/26 May 2004
3-D currents	mooring	ADCP RDI 300 kHz	0–48 m dz=8 m	13 Sep 2003/26 May 2004

OSD

7, 445–475, 2010

Table 2. General statistics of currents: mean East and North components with standard deviation, resulting intensity and direction; mean velocity magnitude with standard deviation and maximum for each level.

	8 m	16 m	24 m	32 m	40 m	48 m
East ($cm\,s^{-1}$)	−5.3	−5.7	−5.3	−5.0	−4.7	−4.6
Std	15.4	13.8	12.7	11.6	10.7	9.6
North ($cm\,s^{-1}$)	8.7	11.3	10.8	9.9	9.0	8.2
Std	14.7	12.4	11.4	10.4	9.3	8.4
Intensity ($cm\,s^{-1}$)	10.2	12.6	12.0	11.1	10.1	11.3
Direction (° N)	328	333	334	333	332	330
Velocity magnitude ($cm\,s^{-1}$)	20.8	19.7	18.3	16.9	15.4	13.9
Std	11.3	11.0	10.0	9.1	8.2	7.7
Max	82.7	63.1	56.8	52.8	49.7	42.8

OSD
7, 445–475, 2010

Table 3. Complex correlation coefficient matrix: absolute values in the lower-left part, angles in the upper-right.

Angle (°) abs	8 m	16 m	24 m	32 m	40 m	48 m
8 m		2.3	4.4	5.8	6.4	4.7
16 m	0.80		2.5	4.0	4.5	3.6
24 m	0.74	0.97		2.2	3.0	2.8
32 m	0.67	0.88	0.95		1.5	2.8
40 m	0.60	0.80	0.85	0.95		3.0
48 m	0.55	0.71	0.77	0.86	0.95	

OSD

7, 445–475, 2010

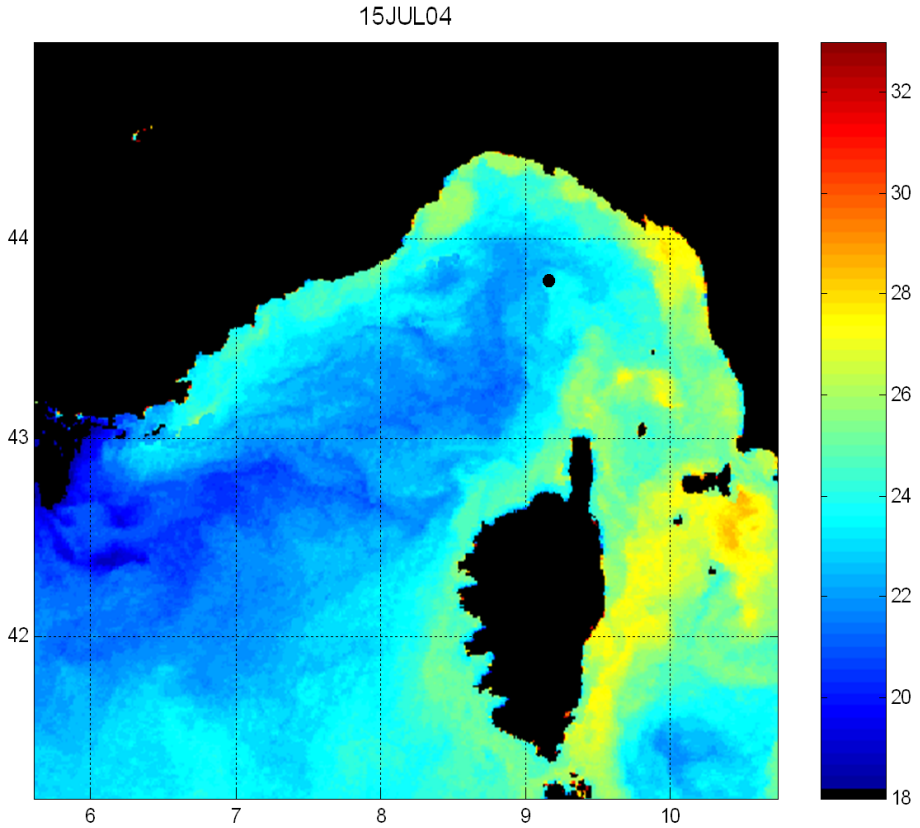

Fig. 1. SST of the Ligurian Sea evidencing the front separating the peripheral coastal waters from the waters of the central zone. A dot marks the location of the ODAS ITALIA1 buoy and the mooring.

OSD
7, 445–475, 2010

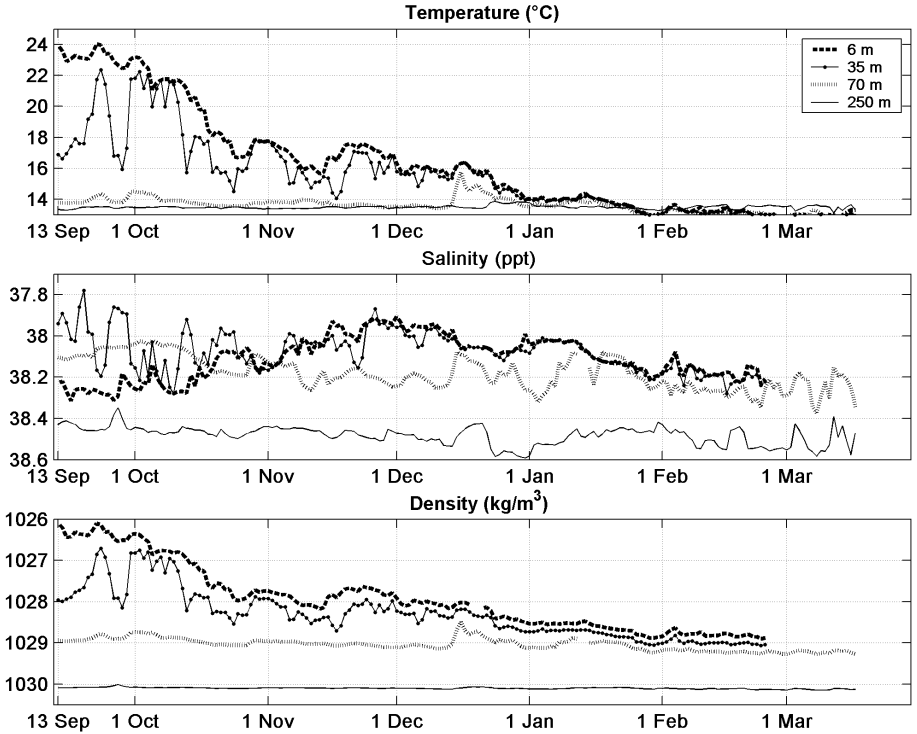

Fig. 2. Time series of sea temperature, salinity and density from 13 September 2003 to 8 March 2004 at 5 m, 36 m, 68 m, and 250 m depth.

OSD
7, 445–475, 2010

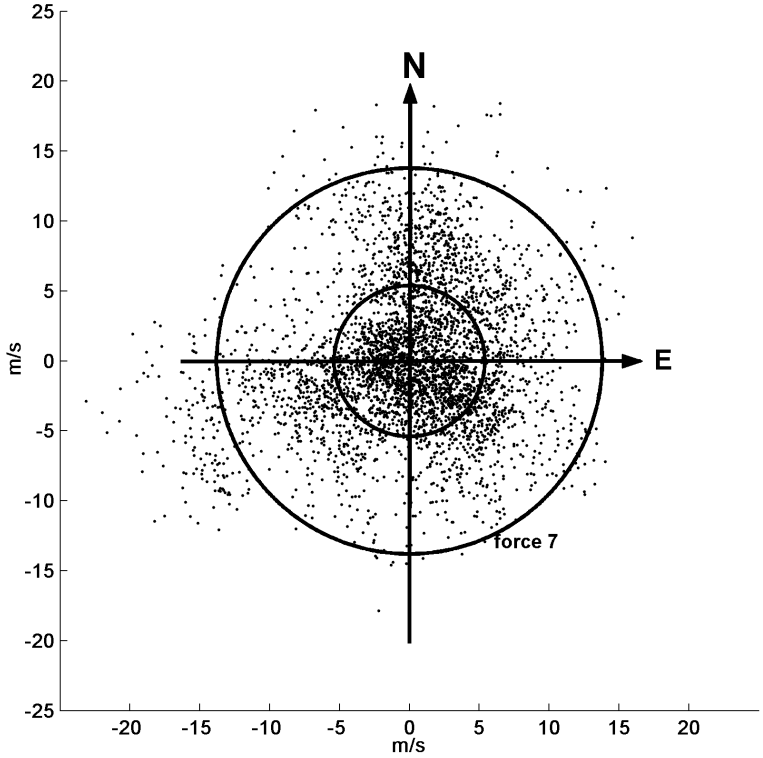

Fig. 3. Scatter plot of hourly data of wind speed.

OSD

7, 445–475, 2010

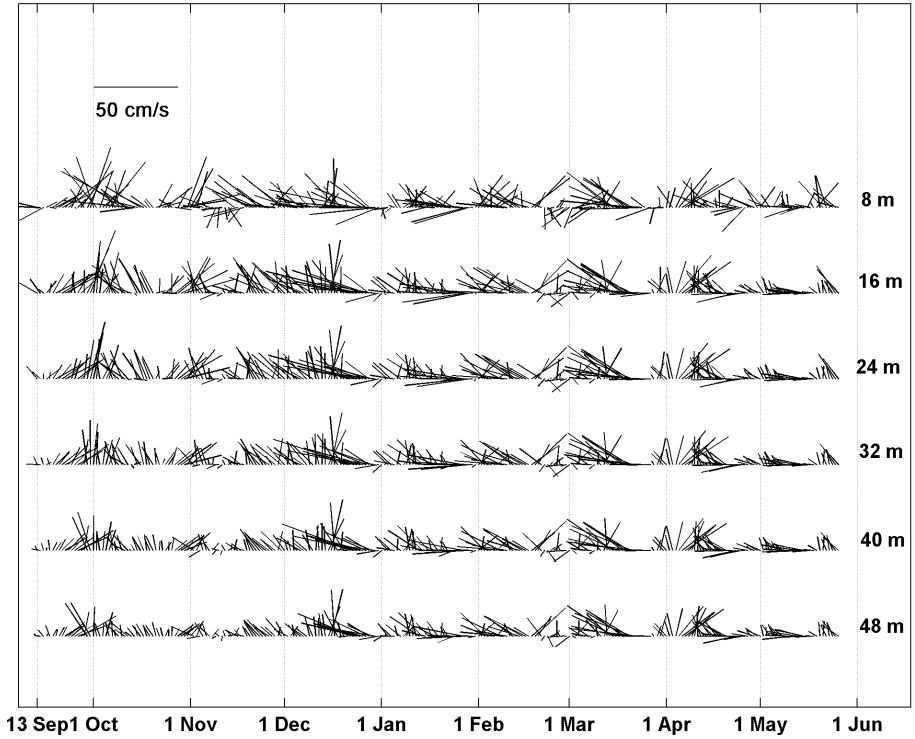

Fig. 4. Stick diagram of daily mean data of horizontal currents from the ADCP.

OSD
7, 445–475, 2010

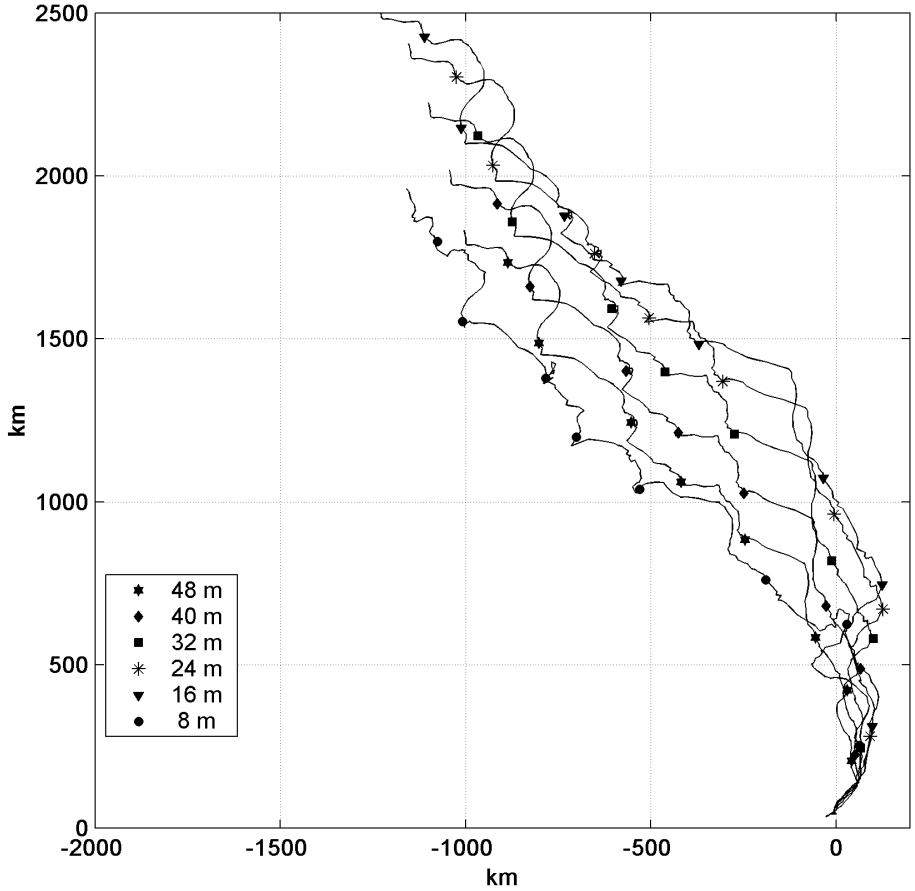

Fig. 5. Progressive vector of daily mean data of currents. Markers 1st of each month.

OSD
7, 445–475, 2010

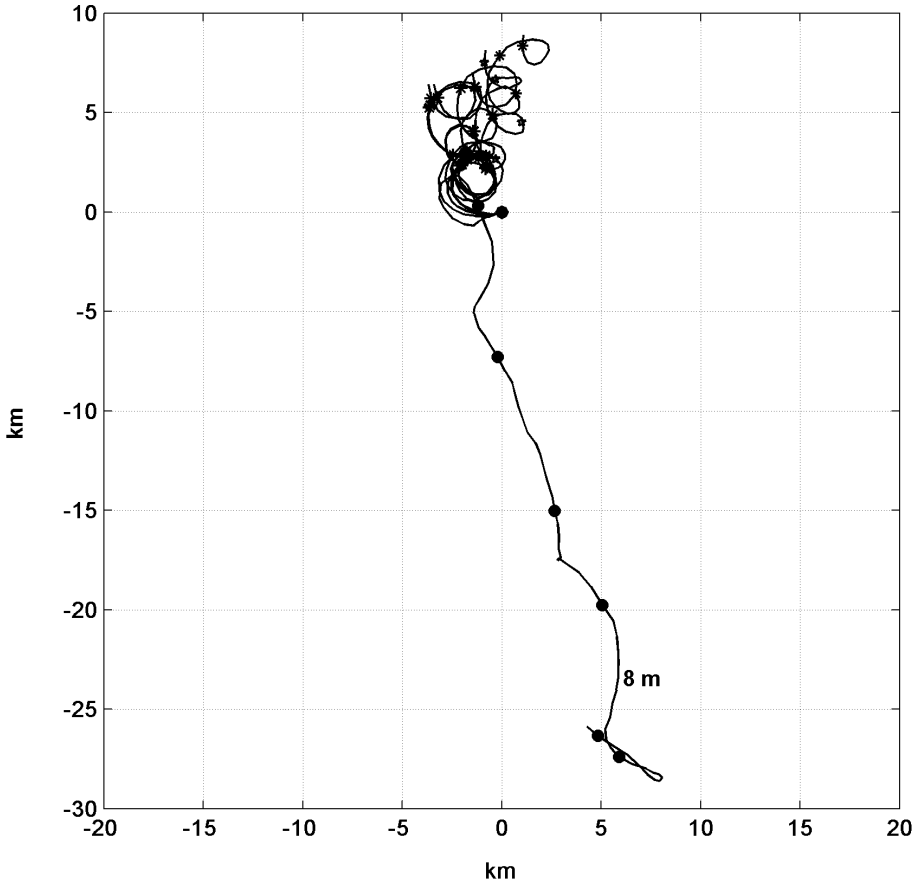

Fig. 6. Progressive vector of hourly data of currents from 9 to 15 November. Markers each 12 h.

OSD

7, 445–475, 2010

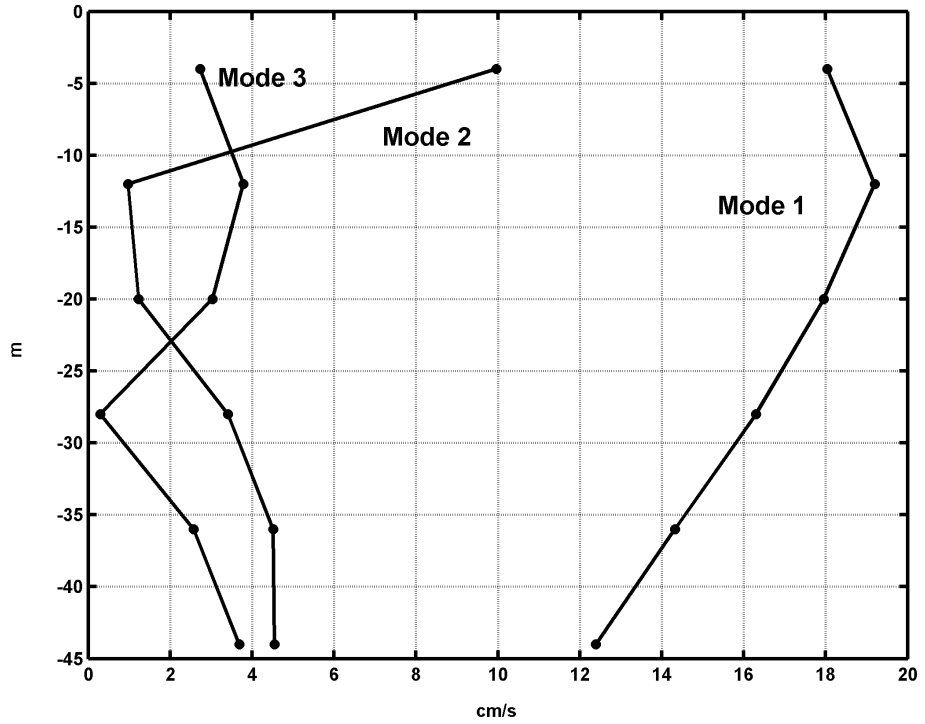

Fig. 7. Vertical profile of the first three EOF modes magnitude.

OSD
7, 445–475, 2010

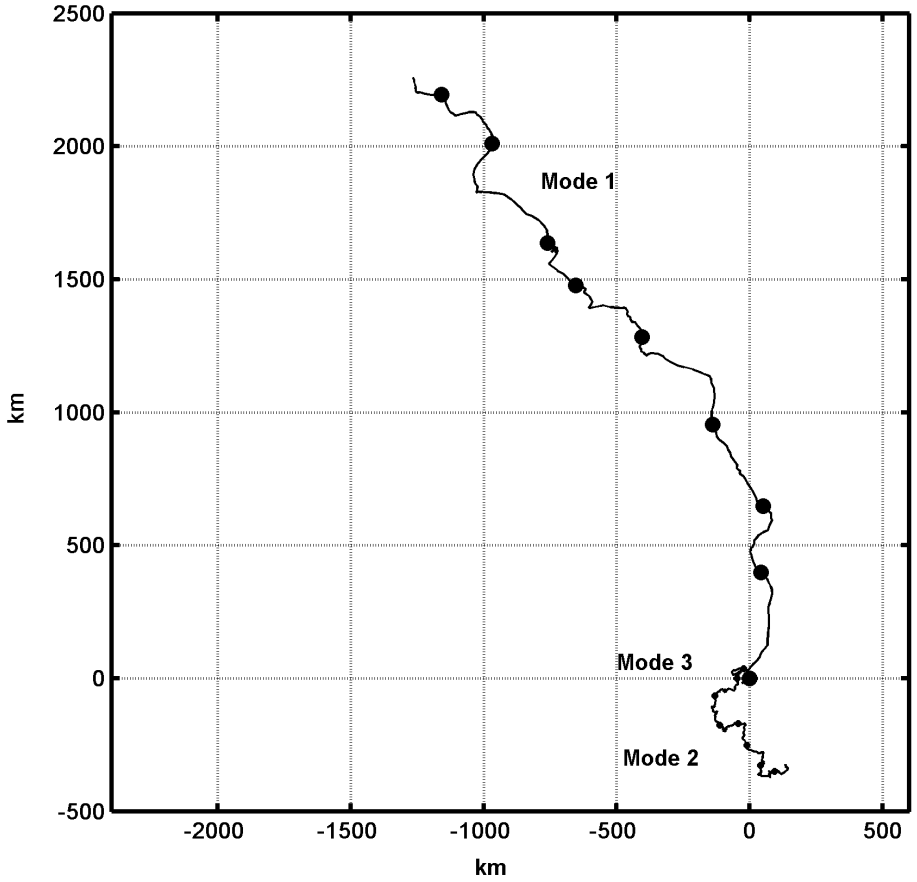

Fig. 8. Progressive vector of the first three EOF modes currents in the upper layer. Markers 1st of each month.

OSD
7, 445–475, 2010

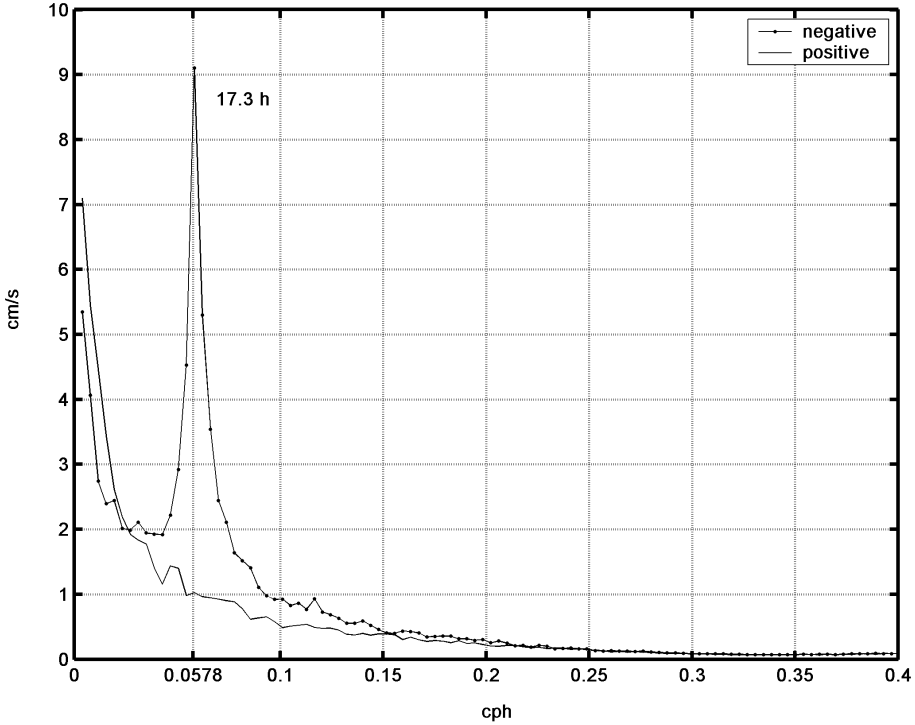

Fig. 9. Vertically averaged Rotary Spectrum of currents.

OSD
7, 445–475, 2010

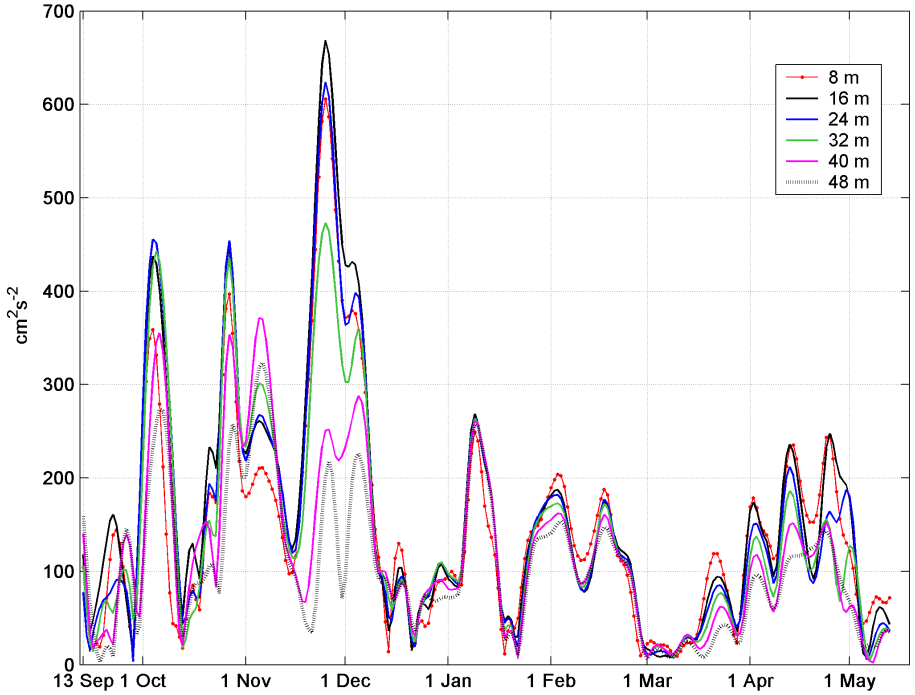

Fig. 10. Smoothed time series of energy on the inertial band extracted from the spectrogram.

OSD
7, 445–475, 2010

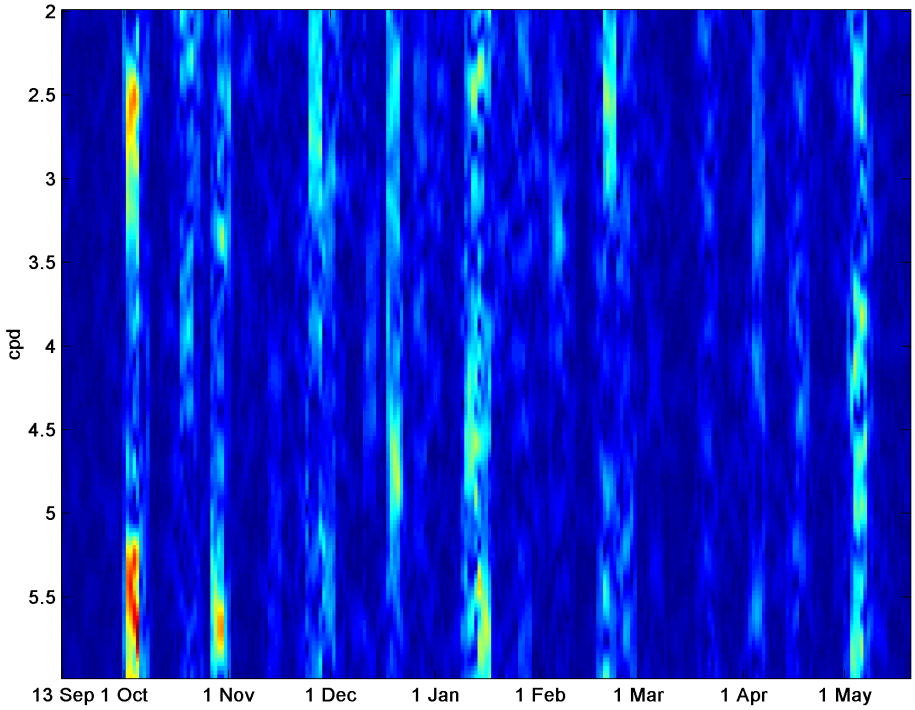

Fig. 11. Time/frequency distribution of amplitude of vertical currents at 16 m depth.

OSD
7, 445–475, 2010

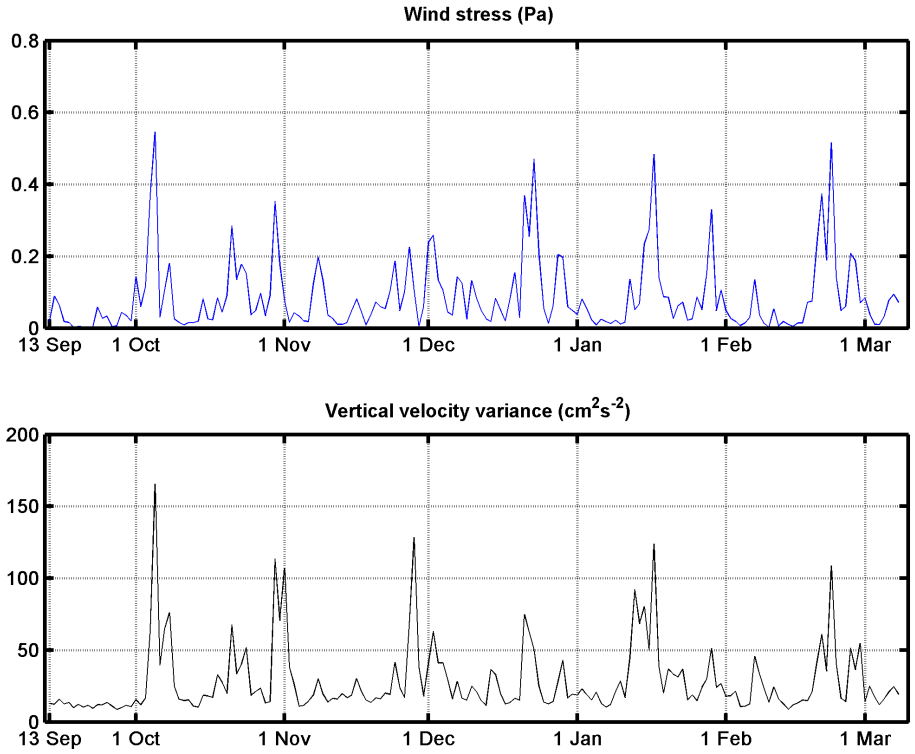

Fig. 12. Time series of daily mean wind stress magnitude and vertical velocities standard deviation.

OSD
7, 445–475, 2010